Chemical Engineering Science 190 (2018) 297–311

Contents lists available at ScienceDirect

Chemical Engineering Science

journal homepage: www.elsevier.com/locate/ces

Reactive distillation with pervaporation hybrid configuration for enhanced ethyl levulinate production

Felicia Januarlia Novita [a], Hao-Yeh Lee [b,*], Moonyong Lee [a,*]

[a] School of Chemical Engineering, Yeungnam University, Dae-dong 712-749, Republic of Korea
[b] Department of Chemical Engineering, National Taiwan University of Science and Technology, Taipei 10607, Taiwan

HIGHLIGHTS

- A novel RD combined with PV process was proposed for enhanced LAEE production.
- The excess EtOH reactant showed a significant advantage over the excess LA case.
- The proposed hybrid configuration reduced the energy and TAC remarkably.
- Thermal coupling enhanced the efficiency of the hybrid process successfully.
- Series PV arrangement was suitable for LAEE production process.

GRAPHICAL ABSTRACT

Thermally coupled reactive distillation-pervaporation ($TCRD_{SS}$-PV) hybrid configuration saves the energy requirement of LAEE production process remarkably up to 73.0%.

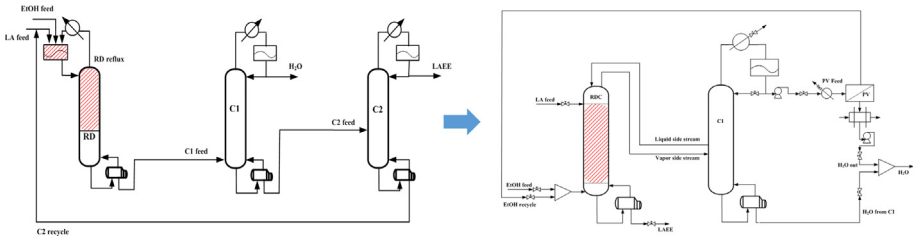

ARTICLE INFO

Article history:
Received 10 May 2017
Received in revised form 7 June 2018
Accepted 9 June 2018
Available online 18 June 2018

Keywords:
Ethyl levulinate production
Reactive distillation-membrane hybrid process
Thermally coupled reactive distillation
Pervaporation membrane arrangement
Excess reactant
Energy efficiency

ABSTRACT

A hybrid process design based on reactive distillation (RD) combined with pervaporation membrane systems was proposed for the production of ethyl levulinate (LAEE) via esterification. In the proposed hybrid configuration, LAEE is produced from the bottom stream of the RD column while the ethanol/water mixture from the overhead is fed to an additional column. The azeotropic mixture in the overhead of the additional column is separated in the pervaporation unit, and the ethanol-rich stream is recycled to the RD column. An RD-only configuration with excess ethanol reactant was also examined to investigate the benefit of excess ethanol reactant and the azeotrope mixture separation. The proposed RD with pervaporation hybrid configuration provided 61.0% and 71.0% reductions of the total annual cost and energy, respectively, compared to the conventional RD configuration with excess levulinic acid (LA) reactant and 6.0% and 13.0%, respectively, as compared to the conventional RD configuration with excess ethanol reactant. The results demonstrated the advantage of the proposed hybrid RD process using pervaporation for lowering the cost and improving the energy efficiency of LAEE production. Different pervaporation arrangements (such as series and parallel arrangements) were discussed in connection with the two main variables (operating temperature and concentration gradient) affecting the membrane flux. The series arrangement was more suitable for the LAEE hybrid process because the influence of the operating temperature is dominant in this process. Thermal intensification in the RD-pervaporation was also examined for exploring further energy reduction. This thermally coupled RD-pervaporation hybrid configuration

Abbreviations: LAEE, ethyl levulinate; LA, levulinic acid; PV, pervaporation; RD, reactive distillation; RD_{LA}, reactive distillation using an excess LA reactant; $RDEt_{OH}$, reactive distillation using an excess EtOH reactant; TAC, total annual cost; TCD, thermally-coupled distillation; TCRD, thermally-coupled reactive distillation; $TCRD_{SS}$, thermally-coupled reactive distillation with a side-stripper; $TCRD_{SS}$-PV, thermally-coupled reactive distillation−pervaporation.

* Corresponding authors.
E-mail addresses: haoyehlee@mail.ntust.edu.tw (H.-Y. Lee), mynlee@yu.ac.kr (M. Lee).

https://doi.org/10.1016/j.ces.2018.06.024
0009-2509/

provided further reductions in total annual cost and energy by 63.0% and 73.0%, respectively, compared to the conventional RD configuration with excess LA reactant.

1. Introduction

Ethyl levulinate (LAEE), which is one of main derivatives of levulinic acid (LA), has attracted considerable interest as a next-generation fuel additive with its many advantages such as higher engine efficiency and lower CO and NO_x emissions (Fagan and Manzer, 2006; Joshi et al., 2011). The global LAEE market is expected to reach USD 11.8 million by 2022 (Grand View Research, 2016). Because the global LAEE industry is still in its nascent stage, research has focused primarily on R&D for a novel commercial LAEE production technology. Unlu and Hilmioglu (2016) mentioned that the synthesis of LAEE can be generally carried out using a homogeneous catalyst in a conventional batch reactor. However, Huber et al. (2006) reported that ester levulinates, including LAEE, are normally produced in two reaction steps: LA is dehydrated to angelica lactone and then mixed with an alcohol to form levulinate. However, the two reaction steps make the process complicated and expensive. To address the problem associated with the two reaction steps, Nandiwale et al. (2013) carried out an esterification experiment, in which LA reacted directly with alcohol to form levulinates. Because the esterification process is a reversible reaction where high conversion can only be achieved if the backward reaction is minimized, they employed excess ethanol (EtOH) to reach the high conversion of LA in the esterification reaction. Recently, to overcome the equilibrium limitation in the esterification of LA more efficiently, Novita et al. (2017) applied a reactive distillation (RD) technique to the LAEE production process and proposed several reactive distillation configurations with excess LA reactant.

Reactive distillation is an important example of combined reaction and separation in a single column, and is especially useful for equilibrium-limited reaction systems (Buchaly et al., 2007; Taylor and Krishna, 2000). Reactive distillation offers numerous advantages, such as improved yield and selectivity, decreased energy requirements, and avoidance of hot spots (Novita et al., 2015). These advantages are promising for the application of reactive distillation columns in esterification, where the conventional process has an equilibrium limitation and high operating costs.

Thermally-coupled distillation (TCD), where either the condenser or the reboiler, or both, in one column are replaced by additional thermal links (an interconnecting vapor liquid stream) to the other columns, is an attractive alternative that offers lower energy consumption in distillation processes (Triantafyllou and Smith, 1992). Both reactive distillation and thermally-coupled distillation are further developments of the conventional distillation unit (Wang et al., 2010) but represent two different methods of integration. However, reactive distillation and thermally-coupled distillation can be combined to create a new process integration concept termed "thermally-coupled reactive distillation" (TCRD). By implementing thermally-coupled reactive distillation, the advantages of both processes (reactive distillation and thermally-coupled distillation) can be harnessed and enhanced, and further cost reduction is possible compared to the conventional distillation unit. In particular, thermally-coupled reactive distillation is suitable to particular reaction-separation systems in which the unreacted components and products are integrated in at least a ternary mixture (Galindo et al., 2011).

Along with the distillation system, membrane systems are now recognized as a possible alternative to traditional energy intensive separation methods such as distillation. Membrane systems often offer lower capital and utility costs and can be used for a wide range of separations (Verhoef et al., 2008). Pervaporation (PV) membrane is most suitable if the liquid mixtures form an azeotrope or contain thermally-unstable components and/or have components with close boiling points (Nagai, 2010). In pervaporation, the feed and retentate are in the liquid-state on the high-pressure side of the membrane, while the permeate is removed as a vapor on the low-pressure side of the membrane. Pervaporation has been the subject of many papers for several decades as mentioned by Luyben (2009). As a stand-alone process, pervaporation is probably not economically feasible. However, in a hybrid or combined process, such as when coupled with a distillation unit or a reactor, the overall efficiency of pervaporation can be improved (Lipnitzki et al., 1999; Verhoef et al., 2008; Singh and Rangaiah, 2017). Based on the advantages of membrane and distillation systems, their combination with pervaporation is anticipated to find increasing application in the future (Aiouache and Goto, 2003). Recently, the research effort for distillation-membrane hybrid systems was expanded to combine it with more complicated distillation systems such as thermally coupled and reactive distillation (Lee et al., 2016; Harvianto et al., 2017a, 2017b).

In this paper, a novel hybrid process combining reactive distillation and pervaporation is proposed for the enhanced production of LAEE via esterification. To force the forward reaction in the esterification of LA to LAEE, an LA or ethanol reactant needs to be provided in excess to the reactive distillation column while the product H_2O recycled to the reactive distillation column, if any, is minimized. In the proposed hybrid process, an excess EtOH reactant configuration was chosen to utilize a highly selective membrane unit for EtOH/H_2O separation. A reactive distillation-only configuration with the excess EtOH reactant, where the EtOH/H_2O azeotrope mixture is recycled to the reactive distillation column without further separation, was also examined to investigate the effect of different excess reactants and the azeotrope mixture separation on overall process performance. Thermal intensification was also investigated for exploring further energy and cost reductions in the RD–pervaporation hybrid process. The arrangements of the pervaporation unit are also discussed to highlight its significance in real applications of membrane hybrid configuration.

2. Model development

2.1. Thermodynamic and kinetic models

There are four components in the studied system, i.e., two reactants (EtOH and LA) and two products (LAEE and H_2O). The non-random two liquid (NRTL) model was used to calculate the liquid activity coefficient, and the Hayden and O'Connell (HOC) model was used to account for association in the vapor phase (Novita et al., 2017). The EtOH and H_2O pairing parameters were obtained from the Aspen Plus built-in database, and the remaining parameters refer to the regressed results from Resk's paper (Resk et al., 2014).

The reversible esterification reaction for the studied system is represented as:

$$\underset{(\mathrm{LA})}{C_5H_8O_3} + \underset{(\mathrm{EtOH})}{C_2H_5OH} \underset{k_2}{\overset{k_1}{\Longleftrightarrow}} \underset{(\mathrm{LAEE})}{C_7H_{12}O_3} + \underset{(H_2O)}{H_2O} \quad (1)$$

The kinetic model for the above reaction is obtained from the research studies by Tsai (2014) and Novita et al. (2017). A heterogeneous Amberlyst™ 39 catalyst was used in the study. The nonideal-quasi-homogeneous (NIQH) kinetic model was used to fit the experimental data. The data of this kinetic model, based on the activity, are summarized in Table 1. In the table, R = 8.314 kJ/kmol·K is the gas constant and T (K) is the absolute temperature. Note that the unit of the reaction rate constants is kmol/kg_{cat}/s, which is converted to kmol/m^3/s in the simulation study by assuming a catalyst density of 770 kg/m^3.

2.2. Pervaporation unit

In this study, a commercial simulator, Aspen Plus V8.6, was used to obtain a rigorous simulation. The RadFrac module based on the equilibrium stage model was used to calculate the total material, components, and energy balance in each column. A simple engineering model from Luyben (2009) was adopted to perform a pervaporation unit. A pervaporation model was built up using Aspen Custom Modeler V8.4 software and then integrated into the Aspen Plus V8.6 software.

The dynamics of the membrane model from Luyben (2009) was based on the pervaporation performance curves reported by Sander and Soukup (1988). In Sander and Soukup's report, they clearly discussed about utilizing a highly selective polyvinyl alcohol (PVA) composite membrane as a pervaporation unit for the ethanol dehydration process. In this context a PVA membrane, which has the hydrophilic characteristic that allows the water to pass selectively across the membrane, was chosen in this study. The amount of mass transfer in the membrane depends on the diffusivity of each species. Water has a larger diffusion coefficient than other components because the membrane is hydrophilic.

The curve for the EtOH/H_2O system indicates relationships between three variables, i.e., the flux of H_2O through the pervaporation membrane, the composition of the permeate vapor, and the concentration of EtOH in the liquid feed. The pervaporation model assumes that diffusion through the membrane depends on the concentration difference between the retentate and permeate sides of the membrane for each component:

$$\text{flux}_j = \text{D}_j(\text{C}_{\text{R}j} - \text{C}_{\text{P}j}) \tag{2}$$

where flux_j denotes the molar flux of component j (kmol/h·m^{-2}), D_j is the diffusion coefficient (m/h), C_{Rj} is the concentration of component j in the retentate liquid (kmol/m^3), and C_{Pj} is the concentration of component j in the permeate vapor (kmol/m^3).

Normally, the diffusion coefficient, D_j, is temperature dependent, and can be expressed as the Arrhenius form:

$$\text{D}_i = \text{D}_{i,0}\exp\left(\frac{-\text{E}_i}{\text{RT}}\right) \tag{3}$$

Based on the data from the curve for the EtOH/H_2O system (Sander and Soukup, 1988) and using Eq. (2), Luyben calculated the diffusion coefficient of EtOH and H_2O (Luyben, 2009). In his work, the average values of $D_{H_2O} = 0.0137$ m/h and $D_{EtOH} = 2.4 \times 10^{-5}$ m/h at 373 K were used for calculation of the membrane parameters. The diffusion coefficient used in this study, referenced from Luyben's work, are presented below:

$$D_{H_2O} = 1.158 \times 10^9 e^{-9385/T}$$

$$D_{EtOH} = 2.028 \times 10^6 e^{-9385/T} \tag{4}$$

The flux of each component in each cell was calculated by using Eqs. (2) and (4) given that all compositions and the temperature are known. The NRTL-HOC relationship was used in the PV unit, where the feed in the pervaporation unit consists of EtOH and H_2O only.

Table 1
Kinetic model and parameters for the studied system.

Kinetic model (catalyst)	k_1	K_a
Quasi-homogeneous model (Amberlyst™ 39) $-r_A = k_1\left(a_{LA}a_{EtOH} - \frac{a_{LAEE}a_{H2O}}{K_a}\right)$ $k_1 = 133.33\exp\left[\frac{-37790}{RT}\right]$ $k_2 = 3.077\exp\left[\frac{-36915.37}{RT}\right]$	at T = 353.5 K, $k_1 = 3.47 \times 10^{-4}$ [kmol/kg_{cat}/s]	at T = 353.5 K, $Ka = \frac{K1}{K2} = 32.18$

3. Discussion of process flowsheet

The esterification of LA and EtOH can be classified as Type I_R according to the classification system based on the relative volatilities of the reactants and products presented by Tung and Yu (2007). Moreover, the excess design is preferable for a system with the lightest reactant, type I_R (Lin, 2007). Based on these premises, Novita et al. (2017) proposed a reactive distillation process, which consists of one reactive distillation and two simple columns in series that employs excess LA for enhanced LAEE production. Fig. 1 shows the flowsheet of the reactive distillation process with the excess LA design for the LAEE production process (Novita et al., 2017). This conventional RD-only configuration using LA as the excess reactant (RD_{LA}-only configuration) required a total reboiler duty of 7.77 Gcal/h with a total annual cost (TAC) of \$5.27 × 10^6 to produce 99.5% mole fraction of LAEE.

In the RD_{LA}-only configuration, because the reaction zone is located in the top section of the reactive distillation column and LA was chosen as the excess reactant, no EtOH remained in the product stream. Thus, the azeotrope formed between EtOH and H_2O and the separation associated with the azeotrope mixture was avoided. Chua et al. (2017) studied the effect of different excess reactants for the RD process to produce isopropyl alcohol and showed that using excess H_2O is more economical than using excess propylene, even though the excess H_2O involves an azeotrope in the process.

In this study, a new RD configuration using EtOH as the excess reactant was investigated for enhanced LAEE production. In the case of excess EtOH reactant, the azeotropic EtOH/H_2O mixture, which is difficult to separate, is essentially involved in the process. Two different approaches can be considered to treat this azeotropic EtOH/H_2O mixture: recycling the excess EtOH either without separation or after separation of the azeotropic EtOH/H_2O mixture. The recycling of excess EtOH after removing H_2O is desirable for the esterification reaction because the reverse reaction by H_2O can be minimized. However, the separation of the azeotrope mixture requires additional capital and energy costs. Therefore, there might be a trade-off, and thus the overall process economics of using an excess EtOH reactant will be mainly determined by the availability of an effective way to separate the azeotrope mixture. It is easily expected that use of a conventional distillation system for the separation of the azeotropic EtOH/H_2O mixture through extractive and azeotropic distillation is undesirable because of its high energy and cost-intensive features. Many practical advantages of pervaporation such as less equipment, lower cost, and lower energy requirements, as well as the commercial availability of a high-performance module for alcohol dehydration, prompted investigation into the RD–pervaporation hybrid process using excess EtOH reactant proposed in this study. To investigate the effect of excess EtOH reactant and azeotrope separation on the RD process performance and economics, an RD_{EtOH}-only configuration, where excess EtOH is directly recycled to the RD column without azeotrope separation, was also studied, as discussed in the following sub-section.

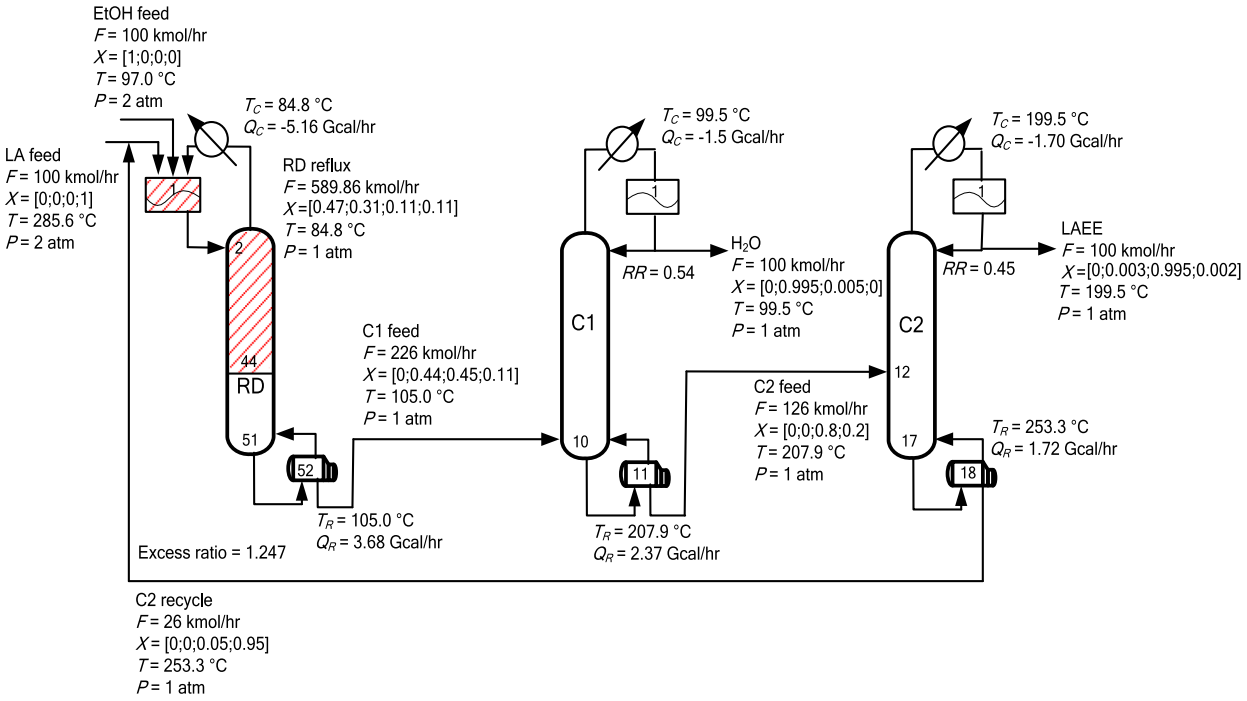

Fig. 1. Flowsheet of the excess LA design for the LAEE production process; X in X_{EtOH}, XH_2O, X_{LAEE}, and X_{LA} denotes the mole fraction (Novita et al., 2017).

3.1. Design and optimization of the RD_{EtOH}-only configuration

Fig. 2 shows the flowsheet of the RD_{EtOH}-only configuration for the LAEE production process. In this RD configuration, because EtOH was selected as the excess reactant, the reaction zone was implemented in the lower section of the reactive distillation column. LA is fed from the third stage and the EtOH mixture is fed from the 32nd stage. In particular, 99.5 mol% of LAEE is produced

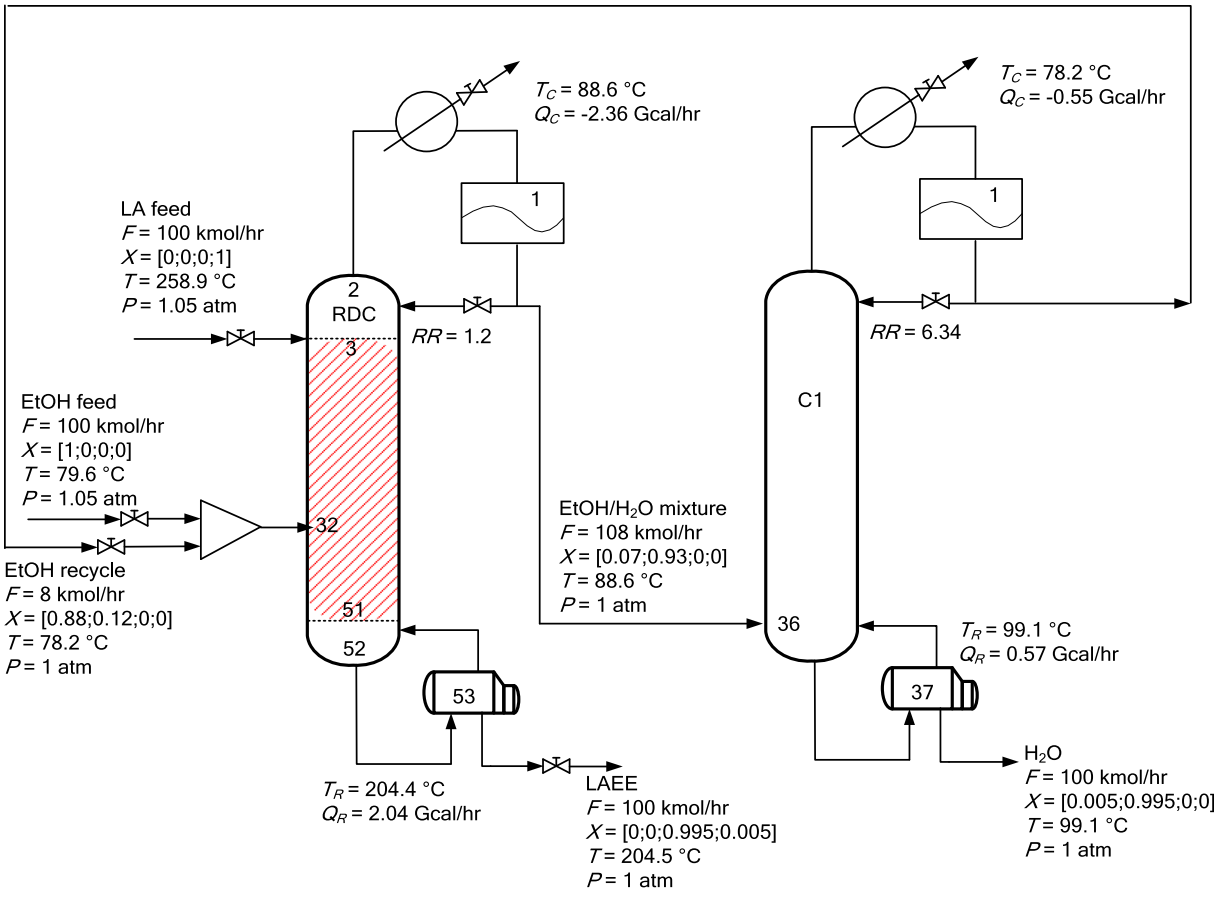

Fig. 2. Flowsheet of the RD_{EtOH}-only configuration; X in X_{EtOH}, XH_2O, X_{LAEE}, and X_{LA} denotes the mole fraction.

from the bottom stream of the RD column with no remaining LA. Moreover, unreacted EtOH and H_2O are obtained as the distillate. The EtOH/H_2O distillate mixture with a mole fraction ratio of 0.07/0.93 is then fed into a subsequent distillation column (C1) for further separation, where pure H_2O is obtained in the bottom stream and a near-azeotropic EtOH/H_2O mixture is obtained in the overhead stream. Note that less H_2O is desirable in the recycled feed to mitigate the reverse reaction. Thus, the near-azeotropic EtOH/H_2O mixture with a mole fraction ratio of 0.88/0.12 is then directly recycled into the reactive distillation column.

The RD_{EtOH}-only configuration was optimized to minimize the total annual cost (TAC) by using an iterative optimization procedure. Note that this sequential optimization procedure does not result in a global optimal solution, but it does give useful insight into the sensitivity of the design variables on the process performance and economics (Novita et al., 2017). Eq. (5) indicates that the payback period (n) for the TAC, which comprises the annual operating cost (AOC) and the annualized total capital cost (TCC), is three years. In this study, the capital cost covers the costs of the column, trays, and heat exchangers (condenser and reboiler), and the operating cost includes the costs of the heating media (the steam or the fuel oil depending on the bottom temperature of the columns), cooling water, refrigerant, and catalyst. The calculation was based on the study by Douglas (1998), ignoring the cost of piping and pumps.

$$TAC = AOC + \frac{TCC}{n} \tag{5}$$

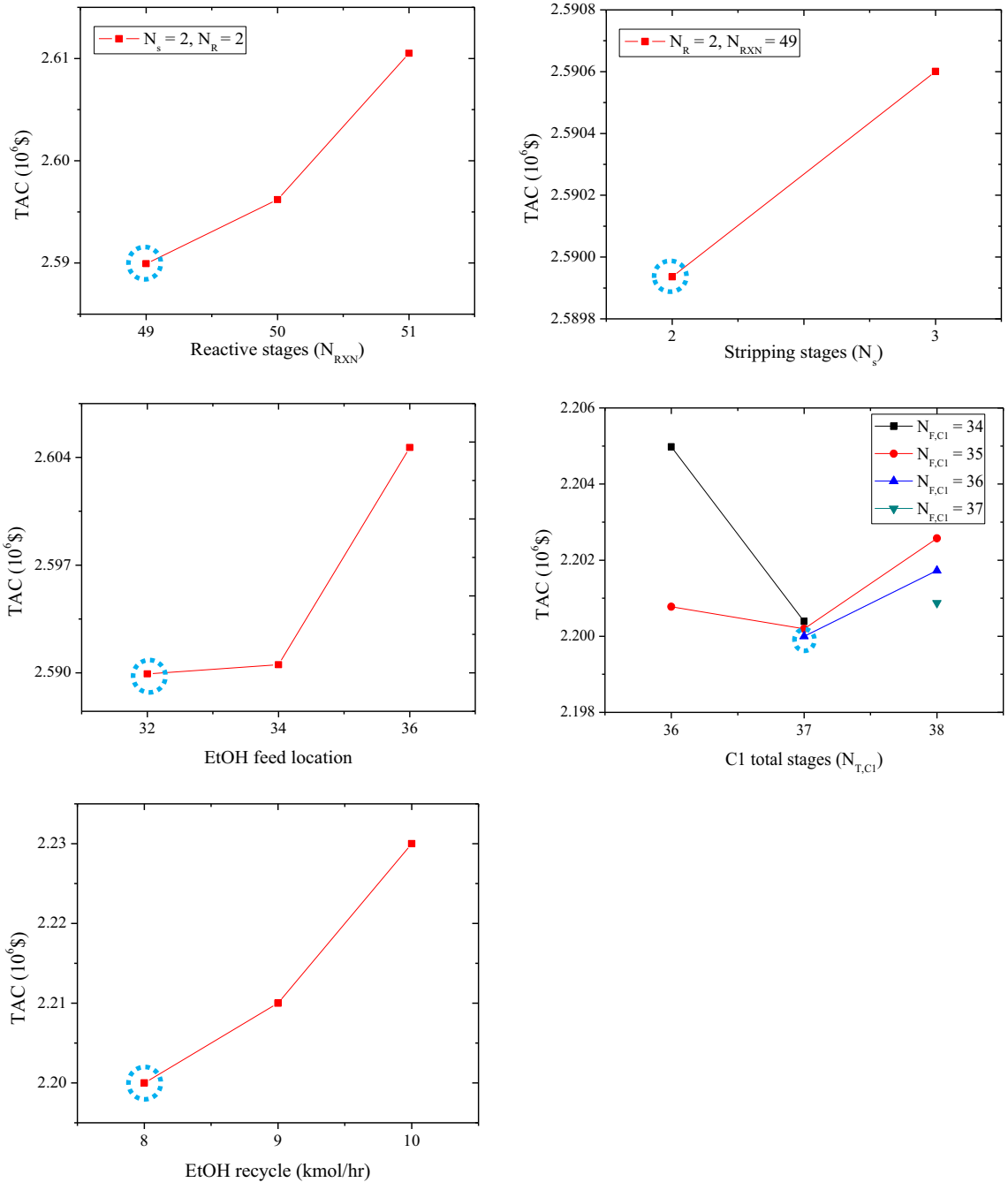

Fig. 3. Sensitivity plots for the main design variables in the column section.

There are six main design variables to be optimized in the column section: (1) the number of reactive stages in the reactive distillation column ($N_{rxn,RD}$); (2) the number of stripping stages in the reactive distillation column ($N_{s,RD}$); (3) the EtOH feed location; (4) the number of stages in C1 (N_{C1}); (5) the C1 feed stage ($N_{F,C1}$), and (6) the EtOH recycling. Fig. 3 presents the sensitivity plots for these variables. The steps used in the iterative optimization procedure for the column section are as follows: (1) Place the heavy reactant feed ($N_{F,LA}$) on the upper part of the reaction section and locate the light reactant feed ($N_{F,EtOH}$) several trays away from the lower part of the reaction section. (2) Fix the number of stripping sections ($N_{s,RD}$). (3) Guess the number of stages in the reactive trays ($N_{rxn,RD}$). (4) Go back to 3 and vary $N_{rxn,RD}$ until the TAC is minimized. (5) Go back to 2 and vary $N_{s,RD}$ until the TAC is minimized. (6) Go back to 1 and vary the $N_{F,EtOH}$ until the TAC is minimized. (7) Fix the number of C1 columns ($N_{T,C1}$). (8) Guess the C1 feed location ($N_{F,C1}$). (9) Go back to 8 and change $N_{F,C1}$ until the TAC is minimized. (10) Go back to 7 and vary $N_{T,C1}$ until the TAC is minimized. (11) Vary the flowrate of recycled EtOH until the TAC is minimized.

Three assumptions were made to design the reactive distillation column in the design procedure (Novita et al., 2017): (1) the downcomer occupies a 10% tray area; (2) the liquid holdup is set as half-full with the Amberlyst™ 39 catalyst in each reactive stage; (3) the weir height is 0.1 m, giving a reactive liquid holdup of 0.069 m^3. In this study, the catalyst cost was also included in the AOC, where the catalyst life was assumed to be three months (Tang et al., 2005; Lee et al., 2016). The column pressures were fixed as 1 atm, the same as in the excess LA reactant process, for the use of cooling water and for fair comparison by excluding the pressure effect on efficiency improvement. The maximum operating temperature of Amberlyst™ 39 is 130 °C, which was considered the main constraint in the design of the reactive distillation column. The reactive distillation column has 53 stages where the reactive stage (i.e., the 3rd to 51th stages) consists of 49 stages. Increasing the number of reactive stages would increase the reactive holdup, which would further reduce the required reboiler duty. However, more stages increase the capital and catalyst cost. As seen from Fig. 3, using a total of 49 reactive stages produced a trade-off between these two competing effects. It should be noted that the number of reactive stages could not be less than 49 because of the maximum allowable temperature limit of the catalyst. The same consideration was applied for the stripping and rectifying stages. These stages could not be less than two for each stage (including condenser and reboiler). The EtOH feed location is also an important variable that can reduce the TAC. Because the EtOH feed exceeds the temperature limit below the 32nd stage, the 32nd stage was chosen as the EtOH feed location. As the number of C1 stages increases, the capital cost increases, but the energy requirement decreases due to the improved separation ability of the C1 column. The optimal number of stages for the C1 column was found to be 37 stages. The optimal feed stage of the C1 column was the 36th stage. A smaller recycle flowrate corresponds to a smaller column diameter and a lower recycling cost. However, at a recycled EtOH flowrate of less than 8 kmol/h, the temperature of the reactive stages exceeds the limit. Figs. 4 and 5 show the temperature and liquid composition profiles, respectively, of the reactive distillation column for the RD_{EtOH}-only configuration. It can be seen from Fig. 4 that the temperature in the reactive stages (the 3rd to 51st stages) is below 130 °C. As a result, the total duty of the RD_{EtOH}-only configuration was 2.61 Gcal/h, with an optimal TAC of $\$2.2 \times 10^6$.

An interesting phenomenon (i.e., a gradual temperature increase while going to the top section) was found from the temperature profile in the reactive section (from the 5th to 50th stages), as seen in Fig. 4, which is impossible in a normal distillation column. In the reactive distillation column, EtOH as

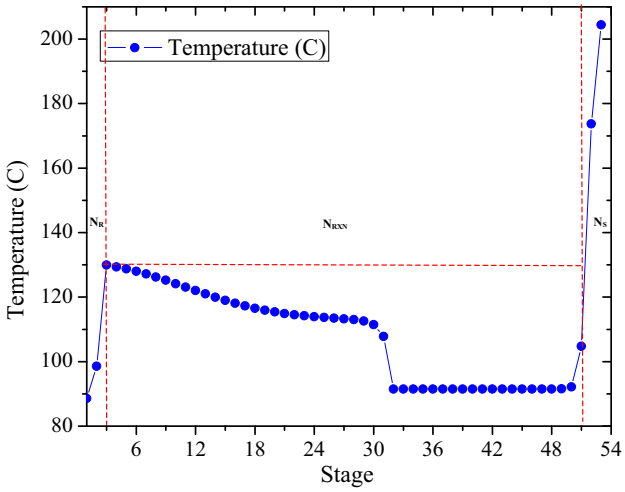

Fig. 4. Temperature profile of the RD column in the RD_{EtOH}-only configuration.

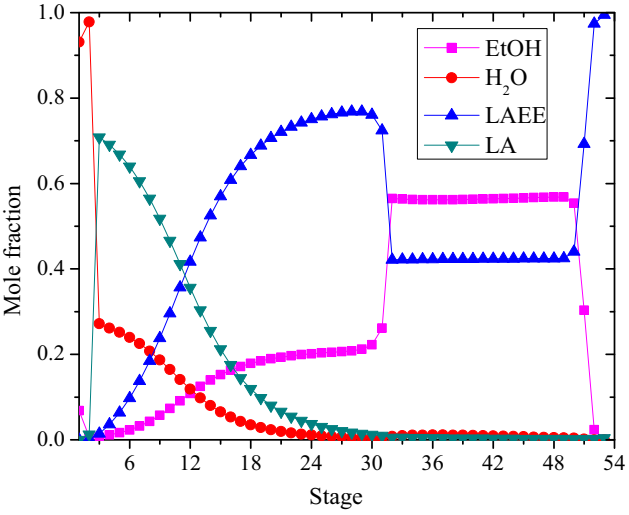

Fig. 5. Liquid composition profile of the RD column in the RD_{EtOH}-only configuration.

the lightest component of the system enters into the lower part of the reactive section (i.e., the 32th stage). As seen in Fig. 5, because of the esterification reaction, its concentration decreases as it travels to the upper section. However, LA, which is the heaviest component of the system, enters into the top part of the reactive section (i.e., the third stage). Its concentration decreases because of the esterification reaction as it travels to the lower section. Both LAEE and H_2O as products are in the middle ranking of those two reactant components and fractionated in the same way as in normal distillation, i.e., the concentration of LAEE, which is heavier than H_2O, increases, whereas the H_2O concentration decreases as it travels to the lower section. The stage temperature of the reactive section is finally determined from this competing effect between feed and product components in the reactive section. As a result, in the RD column for the esterification of LA, a gradual decrease in stage temperature occurred between the 3rd to 32th stages in the reactive distillation section, as seen in Fig. 4. Because very little LA remains by the esterification reaction, whereas only the LAEE and the excess reactant EtOH remain, almost no reaction occurs and a component pinch zone is formed in the reactive distillation zone from the 33th to the 51th stage,

which results in minimal temperature changes in the corresponding stages, as seen in Fig. 4.

3.2. Design and optimization of RD–PV hybrid configuration

In the hybrid configuration combining reactive distillation and pervaporation (the RD–PV hybrid configuration), the near-azeotropic EtOH/H_2O mixture from the overhead of the C1 column is transferred to the pervaporation unit for separation of EtOH from H_2O; the purified excess EtOH is then recycled to the reactive distillation column. Fig. 6 shows a flowsheet of the proposed RD–PV hybrid configuration. The separation task in the columns and the design procedure assumptions were the same as those described in Section 3.1.

An iterative optimization procedure was also applied to this hybrid configuration. Fig. 7 presents the sensitivity plot of the main design variables in the column section for the hybrid configuration. As shown in Fig. 7, the reactive distillation column has the same structure as the RD_{EtOH}-only configuration, i.e., a total of 53 stages with 49 reactive stages (from the 3rd to the 51th stages), whereas the optimal number of stages in the C1 column was found to be 22 stages due to reduced C1 column feed flow. Note that the optimal recycle flowrate in the hybrid configuration could be significantly reduced by up to 6 kmol/h as compared to the RD_{EtOH}-only configuration, which leads to lower capital and operating costs for both the RD and C1 columns. At less than 6 kmol/h, the temperature of the reactive stages exceeds the limit. Fig. 8 shows the temperature profile of the reactive distillation column in the RD–PV hybrid configuration. It can be seen from Fig. 8 that the temperature in the reactive stages remains below 130 °C as the maximum allowable temperature of the catalyst.

As a result, the TAC of the RD-PV hybrid configuration was $\$2.06 \times 10^6$ (comprising the column section: $\$1.97 \times 10^6$ and the membrane section (in series): $\$0.95 \times 10^5$) and the total reboiler duty was 2.28 Gcal/h. The design of the membrane section is discussed in the following subsection.

3.3. Discussion of membrane arrangement

In the membrane separation section, the arrangement of the pervaporation unit is an important design issue. Thus far, to the best of our knowledge, the relationship between the arrangement of the pervaporation unit and the main process variables affecting the membrane flux has not been documented. In this study, the arrangement of the pervaporation unit will be studied as well to determine the best arrangement of the pervaporation unit for this LAEE production process. There are two different basic arrangements of the membrane: parallel and series arrangements (Naidu and Malik, 2011). Fig. 9 shows a schematic of these two arrangements.

In the parallel arrangement, the feed stream is first preheated and split into several streams. Each stream is then sent to the pervaporation unit to meet the product specification in the retentate side via the single module of the pervaporation unit. On the other hand, in the series arrangement, the single feed stream is preheated and sent to the pervaporation unit directly without any splitting. The required product specification is achieved in the retentate side via several pervaporation modules arranged in series.

The membrane flux is an important variable in designing the pervaporation unit because it is closely related to the required membrane area. When the membrane flux increases, the required membrane area decreases. Eqs. (2) and (3) indicate that the concentration gradient and operating temperature are the two main variables affecting the membrane flux.

In this study, both membrane arrangements were investigated under the same inlet conditions. The membrane and the feed conditions in this study have taken from to the work by Luyben (2009), where the mole fraction of the EtOH/H_2O feed mixture was 0.85/0.15 at 101.8 °C. For the maximum temperature tolerated by PVA membrane, Sander and Soukup (1988) stated that it is ultimately determined by the thermal stability of the PVA membrane. In the work by Tsuchiya and Sumi (1969), they reported that the thermal decomposition temperature (T_d) of PVA begins at about

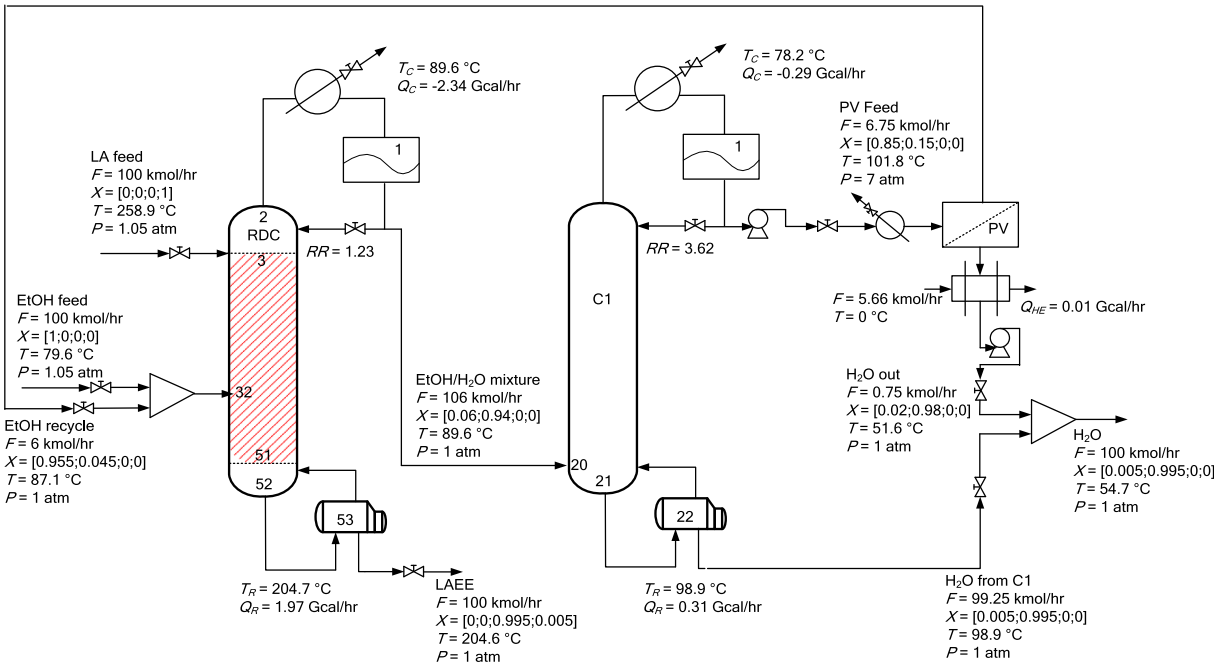

Fig. 6. Flowsheet of the proposed RD-PV hybrid configuration; X in X_{EtOH}, XH_2O, X_{LAEE}, and X_{LA} denotes the mole fraction.

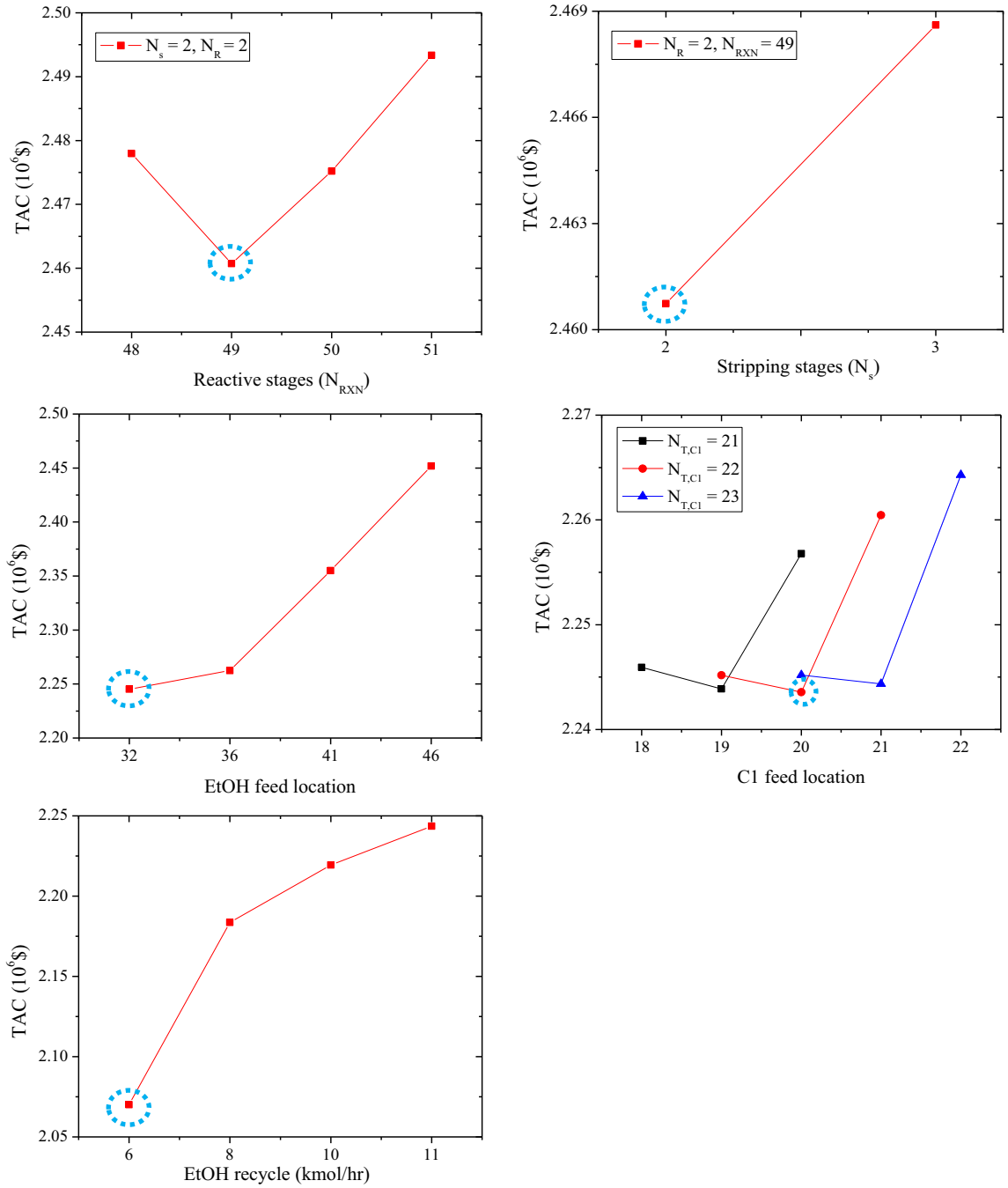

Fig. 7. Sensitivity plot of the main design variables in the column section for the hybrid configuration.

200 °C. Thus, the inlet operating temperature of 101.8 °C is still allowable for PVA membrane. The azeotropic EtOH/H_2O mixture from the C1 column was compressed to a pressure of 7 atm to ensure that the retentate remained in the liquid-phase, and fed into the pervaporation unit. The permeate pressure was 0.155 atm, and the vapor permeate streams from each module were transferred to a refrigerated condenser (with an area of 0.203 m^2 and an overall heat transfer coefficient of 0.0203 cal/s cm^2 K), where the flow rate for condensing the permeate vapor using 0 °C refrigerant was 5.66 kmol/h. The heat duty of the condenser was 0.01 Gcal/h. The retentate flow (6 kmol/h) from the pervaporation unit was fed back into the RD column.

The result showed that the series arrangement with two modules requires a total membrane area of 88 (44 × 2) m^2 to separate the azeotropic EtOH/H_2O mixture. On the other hand, the parallel arrangement requires more modules (three modules) of the pervaporation unit and a larger total membrane area of 348 (116 × 3) m^2. This result illustrates that the arrangement of the pervaporation unit is an important factor that must be considered in the membrane separation section. Note that each module has three cells (or lumps) for both membrane arrangements.

Table 2 presents the details of each membrane arrangement. Notably, the data in Table 2 show that when the parallel arrangement was applied, the H_2O concentration in the feed stream was maintained at the highest value (0.15 mol fraction of H_2O) for all of the pervaporation modules, despite the large temperature drop (ΔT = 36.7 °C). On the other hand, the H_2O concentration in the feed stream decreased gradually in the series arrangement, moving

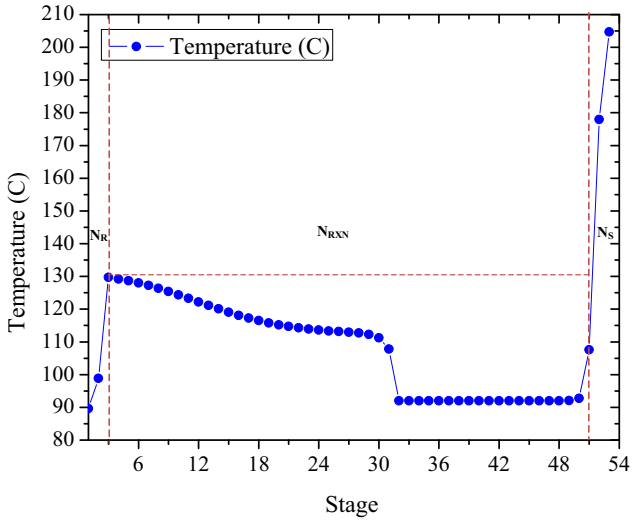

Fig. 8. Temperature profile of the RD column in the hybrid RD-PV configuration.

from a mole fraction of 0.15–0.09. However, the temperature drop (ΔT = 15–20 °C) was smaller than that in the parallel arrangement.

In addition, the simulation results showed that the series arrangement requires a smaller total membrane area than the parallel arrangement because of the larger membrane flux in the former (the membrane flux in the series arrangement was 3.5–5-fold higher than that in the parallel arrangement). These results indicate that in the series arrangement, the influence of the operating temperature is much more important than that of the concentration gradient.

A lower total membrane area also has an economic impact. Fig. 10 shows a cost comparison of both membrane arrangements. The membrane price of 775 US$/m^2 was taken from Szitkai et al. (2002). It was also assumed that one-third of the membrane area need to be replaced each year, on average based on the membrane lifetime of three years (Szitkai et al., 2002). In this study, the membrane price was divided into two parts: (1) the membrane material which has cost per m^2 and (2) the membrane modules which have cost per module (Santoso, 2010; Lee et al., 2016). The capital and operating cost of the vacuum pump were taken from Woods

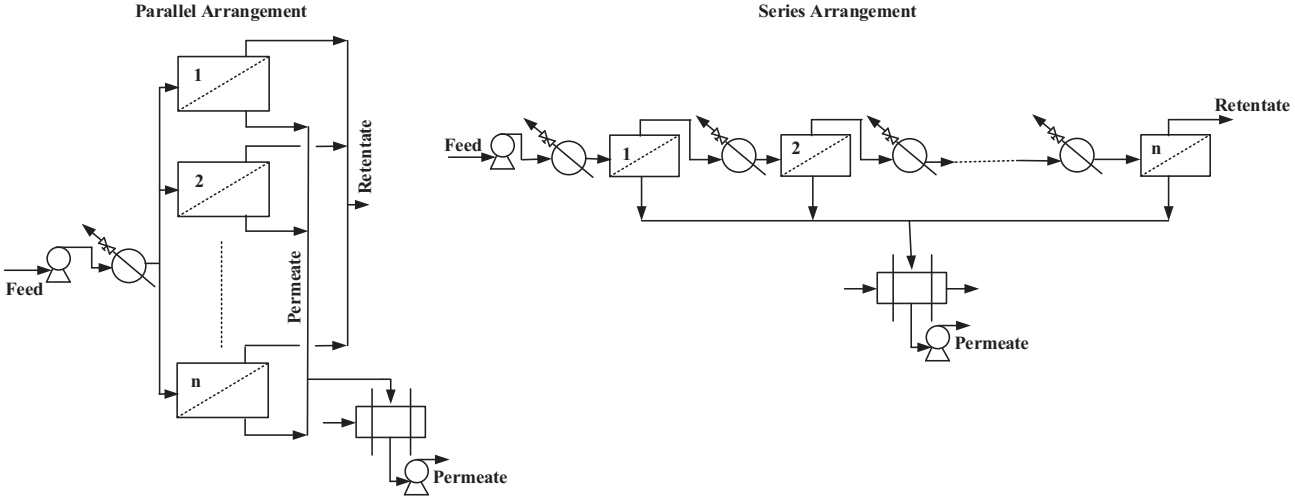

Fig. 9. Schematic of the parallel and series membrane arrangements.

Table 2
Detailed stream information for different membrane arrangements.

	Parallel arrangement						
	Module 1		Module 2		Module 3		
Flux (g/m^2 h)	11.72		11.72		11.72		
Stream type (Feed: F) (Retentate: R)	F	R	F	R	F	R	
Pressure (atm)	7	6.99	7	6.99	7	6.99	
Temp. (°C)	101.8	65.1	101.8	65.1	101.8	65.1	
	Composition (mole fraction)						Out from PV
EtOH	0.85	0.955	0.85	0.955	0.85	0.955	0.955
H_2O	0.15	0.045	0.15	0.045	0.15	0.045	0.045
	Series arrangement						
	Module 1			Module 2			
Flux (kmol/m^2 h)	59.42			41.58			
Stream type (Feed: F) (Retentate: R)	F	R		F	R		
Pressure (atm)	7	6.97		6.97	6.94		
Temp. (°C)	101.8	81.4		101.8	87.1		
	Composition (mole fraction)						Out from PV
EtOH	0.85	0.91		0.91	0.955		0.955
H_2O	0.15	0.09		0.09	0.045		0.045

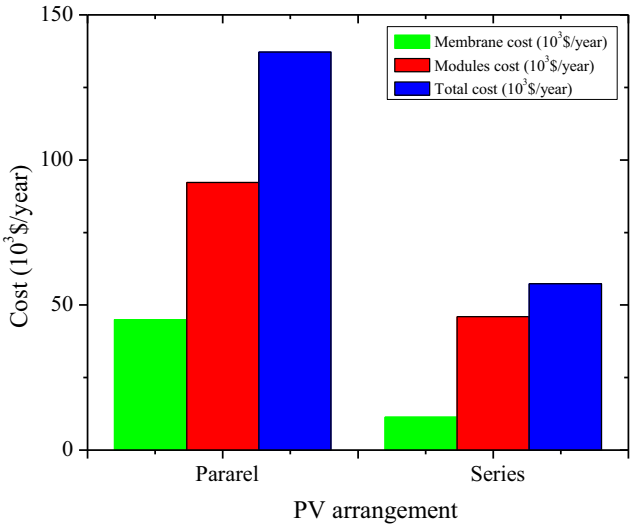

Fig. 10. Comparison of cost effectiveness of both membrane arrangements.

(1983) and Oliveira et al. (2001), respectively. As shown in Fig. 10, for the LAEE hybrid process it turned out that the series arrangement is more economical and suitable than the parallel arrangement. However, in the case where the influence of the concentration gradient is greater than that of the operating temperature, the parallel membrane arrangement can be more adequate.

3.4. Comparison of RD-PV hybrid configuration with the RD_{LA}-only and RD_{EtOH}-only configurations

Table 3 compares the details of the cost distribution of the RD_{LA}-only configuration (Novita et al., 2017), the RD_{EtOH}-only configuration, and the RD–PV hybrid configuration. Although a pervaporation unit is additionally included, the proposed hybrid configuration offers an important advantage derived from the combination of distillation and membrane systems as well as the clever choice of the excess reactant in the reactive distillation design. The total duty (2.28 Gcal/h) and TAC ($2.06 $\times$ 10^6) of the RD–PV hybrid configuration were significantly lower than those of the RD_{LA}-only configuration (total duty 7.77 Gcal/h, TAC = $5.27 $\times$ 10^6) and lower than those of the RD_{EtOH}-only configuration (total duty 2.61 Gcal/h, TAC = $2.20 $\times$ 10^6). Moreover, the RD_{LA}-only configuration had a higher catalyst cost than the RD_{EtOH}-only configuration because of a reactive condenser, for which the holdup was set as the maximum kinetic holdup, which was taken to be 20 times that of the tray holdup (Tung and Yu, 2007; Novita et al., 2017).

In this proposed process configuration, the LAEE (as the heaviest product) exits the reactive distillation column first, and thus, the heaviest reactant, LA, is not present in the product stream, which makes separation in the C1 column much easier. This contribution is clear from the low reboiler duty of the C1 column (0.31 Gcal/h in the proposed hybrid configuration and 0.57 Gcal/h in the RD_{EtOH}-only configuration compared with 2.37 Gcal/h in the RD_{LA}-only configuration). Thus, the separation problem due to the azeotropic mixture could be solved in the most efficient way by embedding the pervaporation unit instead of using additional columns, which also reduces the total duty and total cost of the process: the TAC of the C2 column was $11.48 $\times$ 10^5 in the RD_{LA}-only configuration, whereas the pervaporation unit in series only cost $0.95 $\times$ 10^5.

3.5. $TCRD_{SS}$–PV hybrid configuration

Although the RD-PV hybrid configuration afforded a large improvement in term of TAC and energy saving compared to the RD-only configurations, the process can still be further optimized, especially in terms of energy saving. Fig. 11 shows the liquid

Table 3
Detailed cost distribution of the RD_{LA}-only configuration (Novita et al., 2017), the RD_{EtOH}-only configuration, and the RD–PV hybrid configuration.

Conventional RD_{LA}-only configuration		Conventional RD_{EtOH}-only configuration		RD-PV hybrid configuration	
RD column capital cost ($ 1000/year)					
Column	254.88	Column	258.81	Column	258.81
Trays	49.19	Trays	50.13	Trays	50.13
Heat exchangers	204.53	Heat exchangers	121.58	Heat exchangers	119.92
RD column operating cost ($ 1000/year)					
Catalyst	34.44	Catalyst	1.64	Catalyst	1.64
LP	1791.55	HP	1325.15	HP	1280.31
Cooling water	66.95	Cooling water	30.66	Cooling water	30.45
C1 column capital cost ($ 1000/year)					
Column	62.22	Column	61.98	Column	30.06
Trays	8.19	Trays	6.66	Trays	2.54
Heat exchangers	96.28	Heat exchangers	54.99	Heat exchangers	36.68
C1 column operating cost ($ 1000/year)					
HP	1536.05	LP	279.18	LP	151.82
Cooling water	19.48	Cooling water	7.18	Cooling water	3.82
C2 column capital cost ($ 1000/year)				Pervaporation capital cost ($ 1000/year)	
Column	100.58			Membrane	11.37
Trays	15.18			Modules	45.98
Heat exchangers	113.00			Vacuum pump	3.64
				Heat exchangers	3.38
				Feed pump	0.48
C2 column operating cost ($ 1000/year)				Pervaporation operating cost ($ 1000/year)	
Fuel oil	897.15			Membrane replacement	22.73
Cooling water	22.12			LP	4.49
				Electricity	1.12
				Refrigerant	1.80
Total annual cost (TAC) ($ 1000/year)					
5271.79		2197.96		2061.17	

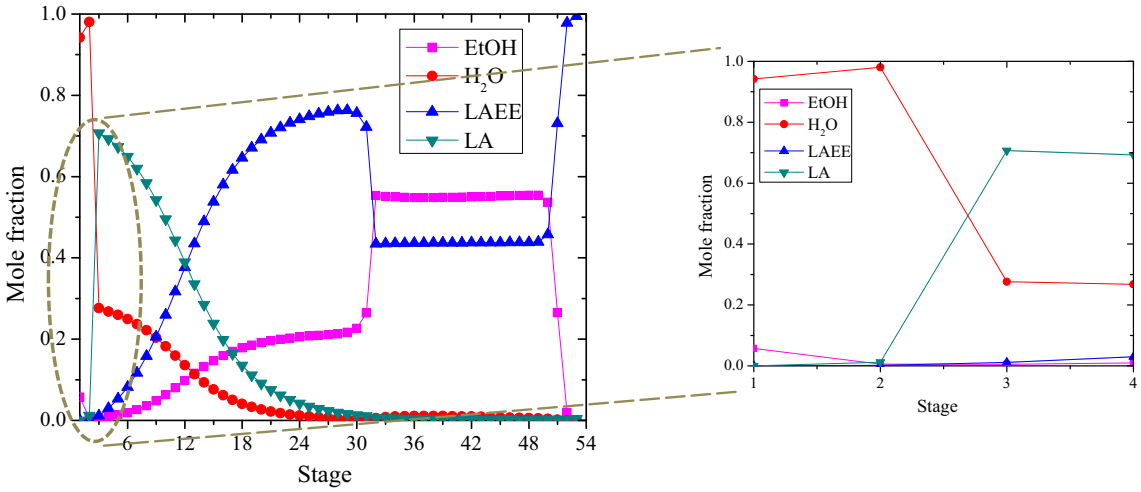

Fig. 11. Liquid composition of the RD column in the RD-PV hybrid configuration.

composition for the reactive distillation column in the RD-PV hybrid configuration.

It can be seen from Fig. 11 that there is a slight remixing effect in the top part of the reactive distillation column. Thus, modifying the column section to the thermally-coupled structure, where one reboiler or condenser, or both, is eliminated and replaced with the interconnecting vapor liquid stream, may possibly offer savings in terms of both energy and capital costs by reducing the remixing effect.

In the proposed hybrid configuration, the apparent remixing effect mostly occurs in the rectifying section of the reactive distillation column. Therefore, thermal links must be placed in the upper section of the column by eliminating one condenser; a thermally coupled reactive distillation with a side-stripper ($TCRD_{SS}$) configuration. Fig. 12 shows the proposed $TCRD_{SS}$-PV hybrid configuration.

Note that the TCRD–PV hybrid configuration was also implemented in the study of Harvianto et al. (2017a) for n-butyl acetate production process. Besides its different application, the structure of the TCRD–PV hybrid configuration used in this study was different from that of Harvianto et al. (2017a,b). Because the pervaporation membrane for EtOH–H_2O separation has a sufficiently high separation performance, no further separation and recycling of the permeate stream from the membrane was required, which makes the hybrid configuration simple and practical.

To focus on the energy saving derived from the column configuration only, the main structures (the total number of stages, etc.,) of the columns and the membrane section in the $TCRD_{SS}$-PV hybrid configuration were kept the same as those in the RD-PV hybrid configuration. In this way, all of the energy saving is derived from the liquid side stream flow rate and the locations of the thermal link feed and EtOH feed. Further improvements in energy efficiency

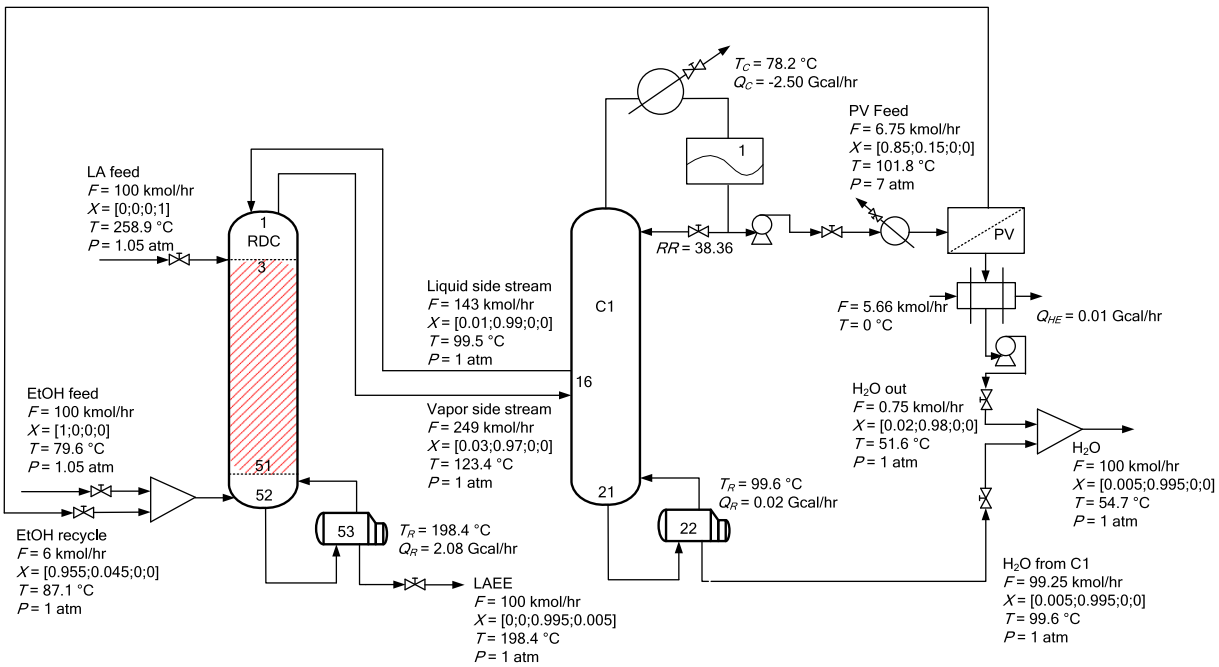

Fig. 12. Flowsheet of the $TCRD_{SS}$ -PV hybrid configuration; X in X_{EtOH}, XH_2O, X_{LAEE}, and X_{LA} denotes the mole fraction.

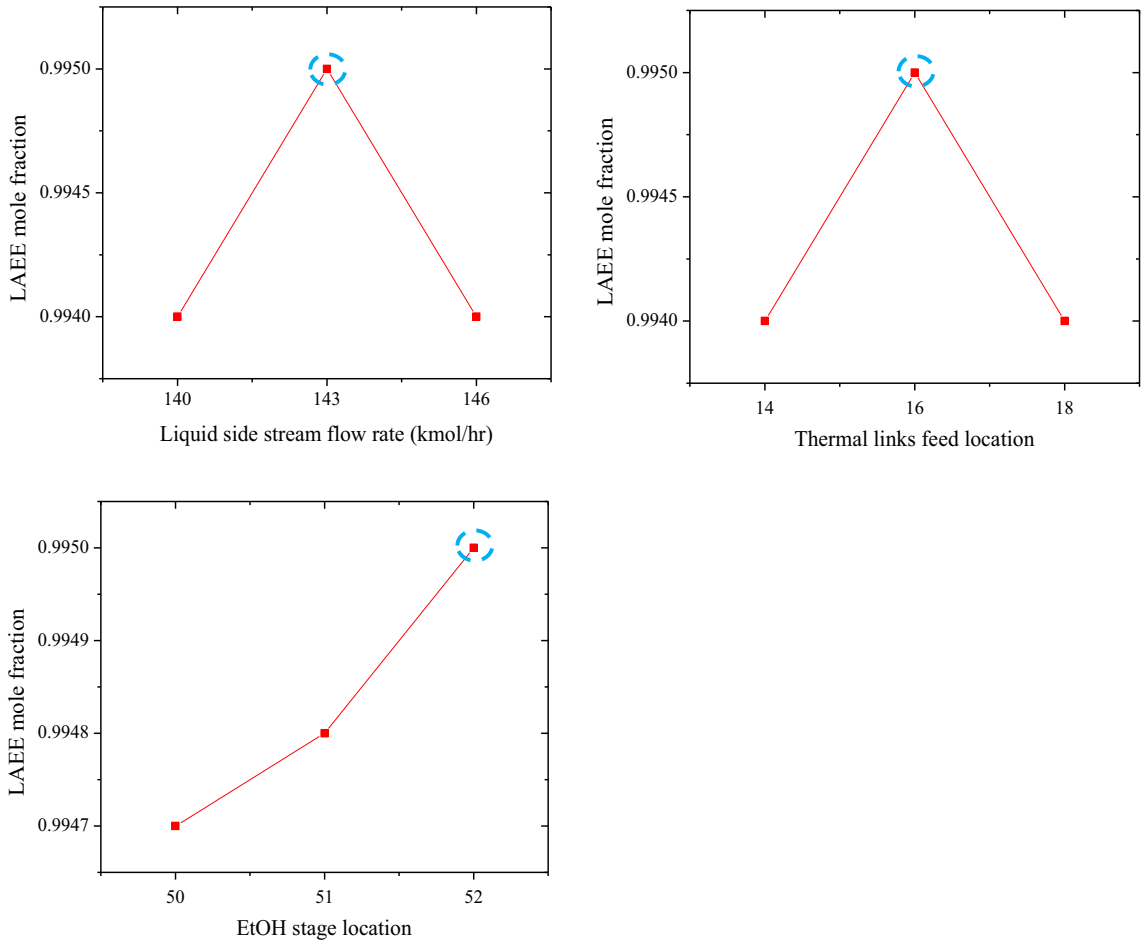

Fig. 13. Effect of three variables in the $TCRD_{SS}$-PV configuration on the production of LAEE (mole fraction).

and cost saving will be possible if the structures of the TCRD and membrane section are fully optimized. Fig. 13 shows the optimization results for these design variables. The optimal liquid side stream flowrate was 143 kmol/h, the location of the thermal link feed was in the 16th stage, and the EtOH feed location was in the 52nd stage. By eliminating one condenser in the reactive distillation column and replacing it with the thermal links, the total duties of the reactive distillation and C1 columns could be reduced by approximately 0.18 Gcal/h.

Fig. 14 shows the liquid composition profile for the reactive distillation column in the $TCRD_{SS}$-PV hybrid configuration. The liquid composition profile at the bottom section of the reactive distillation column was similar to that in the RD-PV hybrid configuration. On the other hand, the remixing phenomenon in the top

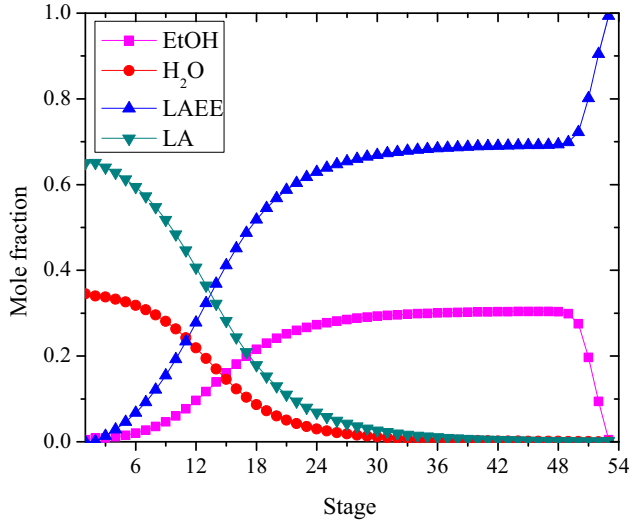

Fig. 14. Liquid composition profile for reactive distillation column in hybrid $TCRD_{SS}$-PV configuration.

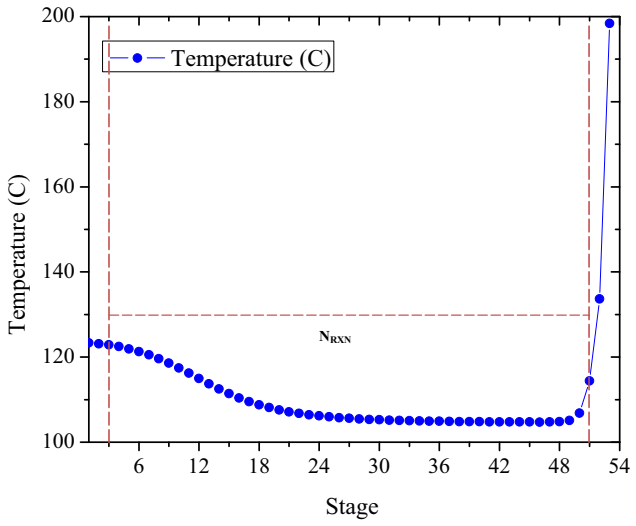

Fig. 15. Temperature profile of the reactive distillation column in the $TCRD_{SS}$-PV hybrid configuration.

Table 4
Comparison of the RD-only, RD-PV hybrid, and $TCRD_{SS}$–PV hybrid configurations.

	Conventional		Hybrid	
	RD_{LA}-only	RD_{EtOH}-only	RD–PV	$TCRD_{SS}$–PV
Total duty (Gcal/h)	7.77	2.61	2.28	2.10
TAC ($)	5.27×10^6	2.20×10^6	2.06×10^6	1.97×10^6
Energy saving (%)		66.0	71.0 (13.0[a])	73.0 (8.0[b])
TAC (%)		58.0	61.0 (6.0[a])	63.0 (4.0[b])

[a] Compared to the RD_{EtOH}-only configuration.
[b] Compared to the RD–PV hybrid configuration.

section of the reactive distillation column was removed. Consequently, the total energy requirement of the $TCRD_{SS}$-PV system was 2.10 Gcal/h, which is equivalent to energy savings of around 8.0% compared to the RD-PV hybrid configuration. Note that the temperature in the reactive section is far under the limit of the catalyst (Fig. 15). The $TCRD_{SS}$-PV hybrid configuration had a TAC of $\$1.97 \times 10^6$ (column section: $\$1.88 \times 10^6$ and membrane section (in series): $\$0.95 \times 10^5$), which is equivalent to a TAC savings of 4.0% compared to the RD-PV hybrid configurations. Table 4 summarizes the design results for the two RD-only and the two hybrid configurations.

4. Conclusions

In this study, hybrid configurations combining reactive distillation and membrane systems were proposed for enhanced LAEE production. The RD-PV hybrid configuration utilizes two columns in sequence combined with the series-pervaporation arrangement. The selection of EtOH as an excess reactant for reactive distillation resulted in a remarkable reduction in the required energy of the subsequent column. Consequently, the proposed RD_{EtOH}-only configuration resulted in significant savings in the TAC and total duty of as much as 58.0% and 66.0%, respectively, as compared to the RD_{LA}-only configuration. In the proposed RD–PV hybrid configuration, the pervaporation unit was successfully utilized to separate the azeotropic EtOH/H_2O mixture in the most efficient way, achieving further savings in the TAC and energy of as much as 6.0% and 13.0%, respectively, as compared to the RD_{EtOH}-only configuration.

Membrane arrangement for the pervaporation units was also an important design factor in the membrane hybrid application. The operating temperature and concentration gradients are the two main design variables affecting the diffusion rate of the membrane. In the proposed hybrid configuration, because the operating temperature was more influential than the concentration gradient, the series arrangement was found to be more advantageous than the parallel arrangement. The higher membrane flux in the series arrangement led to a smaller total membrane area. An intensified hybrid configuration utilizing the TCD, i.e., the $TCRD_{SS}$-PV hybrid configuration, was found to be an effective way to enhance the energy efficiency of the RD-PV hybrid configuration. By removing the remixing effect in the top section of the reactive distillation column, the $TCRD_{SS}$-PV hybrid configuration provided a further reduction in the TAC and energy for LAEE production. Thus, the proposed $TCRD_{SS}$-PV hybrid configuration afforded TAC and energy savings of up to 63.0% and 73.0%, respectively, compared to the RD_{LA}-only configuration, and 4.0% and 8.0%, respectively, compared to the RD-PV hybrid configuration. These hybrid configurations can be extended to other similar chemical processes involving esterification reactions and azeotropic mixtures.

Notes

The authors declare no competing financial interest.

Acknowledgements

This study was supported by the Basic Science Research Program through the National Research Foundation of Korea (NRF) funded by the Ministry of Education (2018R1A2B6001566) and by the Priority Research Centers Program through the National Research Foundation of Korea (NRF) funded by the Ministry of Education (2014R1A6A1031189). The authors are also grateful for the support from the Ministry of Science and Technology of Taiwan under grant MOST 104-2221-E-011-149-MY2.

Appendix A. Total annual and membrane costs calculation

The equipment cost estimation follows the procedure of Douglas (1998). A payback period of three years for the exchanger and column is assumed, and a M&S index of 1473.3 (2010, 3rd quarter) is used in the calculation. The utility costs were taken from Turton et al. (2009). The membrane price was taken from Szitkai et al. (2002). The membrane lifetime was assumed as three years during the calculation. In this study, the membrane price was divided into two parts: (1) the membrane material which has cost per m^2 and (2) the membrane modules which have cost per module (Santoso, 2010; Lee et al., 2016). The capital cost and the operating cost of the vacuum pump refer to Woods (1983) and Oliveira et al. (2001), respectively.

A.1. Reboiler heat exchange area (A_R)

The reboiler heat exchange area (A_R) is determined using the following relation:

$$A_R[ft^2] = \frac{Q_R}{U_R \Delta T_R} \tag{A1}$$

where Q_R [BTU/h] is the reboiler duty, the overall heat-transfer coefficient U_R is assumed 250 BTU/(h ft^2 °F), and the temperature driving force ΔT_R [°F] in the reboiler depends on the steam (for a high bottom temperature that cannot use a high pressure steam, it is used a fuel oil and ΔT_R is assumed 45 °F).

A.2. Condenser heat exchange area (A_C)

The condenser heat exchange area (A_C) can be calculated using the expression,

$$A_C[ft^2] = \frac{Q_C}{U_C \Delta T_C} \tag{A2}$$

where Q_C [BTU/h] is the condenser duty, the overall heat-transfer coefficient U_C is assumed 150 BTU/(h ft^2 °F), and ΔTc is given by

$$\Delta T_C = \frac{120 - 90}{\ln\left(\frac{T_b - 90}{T_b - 120}\right)}$$

with T_b being the condenser operating temperature (in °F).

A.3. Height of column (L_C)

The column height (L_C) is calculated assuming 2-ft tray spacing and allowing 20% more height for base level volume:

$$L_C\ [\text{ft}] = 2.4N_T \tag{A3}$$

where N_T is the total number of trays in the column.

A.4. Cost of column

The column cost is given by the expression

$$\text{column cost}[\$] = \frac{M\&S}{280} \times 101.9 \times D_C^{1.066} \times L_C^{0.802} \times (2.18 + 3.67) \tag{A4}$$

A.5. Cost of tray

The tray cost in the distillation columns can be defined as

$$\text{tray cost}[\$] = \frac{M\&S}{280} \times 4.7 \times D_C^{1.55} \times L_C \times (1 + 1.8 + 1.7) \tag{A5}$$

A.6. Cost of heat exchanger

The following expression is used to determine the heat exchanger cost,

$$\text{heat exchanger cost}\ [\$] = \frac{M\&S}{280} \times 101.3 \times A^{0.65}(2.29 + Fc) \tag{A6}$$

where Fc is 5.0625 for the reboiler and 3.75 for the condenser.

A.7. Utility costs

Utility type	Cost ($/GJ) (by Turton et al., 2009)
Cooling water	0.354
Low pressure steam (LP) (5 barg, 160 °C)	13.28
Medium pressure steam (MP) (10 barg, 184 °C)	14.19
High pressure steam (HP) (41 barg, 254 °C)	17.70
Fuel oil	14.2
0 °C refrigerant	4.92

A.8. Cost of membrane material

$$\text{Membrane material cost}\ [\$] = 387.5/\text{m}^2 \tag{A7}$$

A.9. Cost of membrane module

$$\text{Membrane module cost}\ [\$] = 125550 \times \left(\frac{A}{324}\right)^{0.3} \tag{A8}$$

where A [m^2] is membrane area for each module.

A.10 Cost of membrane replacement

The membrane replacement cost is taken from Szitkai et al. (2002) as 775 US$/$m^2$. In this study, the membrane life time is assumed as 3 years. Therefore, one-third of the total membrane area has to be replaced each year, on average.

A.11. Cost of vacuum pump

$$\text{vacuum pump cost}\ [\$] = 4200 \times \frac{CEPCI10}{CEPCI83} \times \left(\frac{60 \times F_p \times 8.314 \times 273.15}{3600 \times 101.325}\right)^{0.55} \tag{A9}$$

where Fp is the total permeate rate through the membrane [kmol/h].

A.12. Cost of feed pump

$$\text{feed pump cost}\ [\$] = 26700 \times \frac{CEPCI10}{CEPCI83} \times \left(\frac{24 \times F_F \times 3600}{50000}\right)^{0.53} \tag{A10}$$

where F_F is the total feed rate to the pump [m^3/s].

A.13. Power of vacuum pump

$$\text{annual cost of power}\ [\$] = 8150 \times 0.04 \times \left\{\left(\frac{F_P 8.314.273.15}{3600}\right)\left(\frac{k_r}{k_r - 1}\right) \times \left[\left(\frac{1.013}{P_{op}}\right)^{(k_r - 1/k_r)} - 1\right]\right\} \tag{A11}$$

where k_r is the heat capacity ratio (1.33). P_{op} is the pressure on the permeate side.

A.14. Catalyst cost (assuming a catalyst life of 3 months)

$$\text{catalyst cost}\ [\$] = \text{catalyst loading}\ [\text{kg}] \times 7.7162\frac{\$}{\text{kg}} \tag{A12}$$

References

Aiouache, F., Goto, S., 2003. Reactive distillation-pervaporation hybrid column for *tert*-amyl alcohol etherification with ethanol. Chem. Eng. Sci. 58, 2465–2477. https://doi.org/10.1016/S0009-2509(03)00116-7.

Buchaly, C., Kreis, P., Gorak, A., 2007. Hybrid separation process-combination of reactive distillation with membrane separation. Chem. Eng. Process.: Process Intensification 46, 790–799. https://doi.org/10.1016/j.cep.2007.05.023.

Chua, W.J., Rangaiah, G.P., Hidajat, K., 2017. Design and optimization of isopropanol process based on two alternatives for reactive distillation. Chem. Eng. Process.: Process Intensification 118, 108–116. https://doi.org/10.1016/j.cep.2017.04.021.

Douglas, J.M., 1998. Conceptual Design of Chemical Processes. McGraw-Hill.

Fagan, P.J., Manzer, L.E., 2006. Preparation of levulinic acid esters and formic acid esters from biomass and olefins. U.S. Patent 7,153,996.

Galindo, E.Y.M., Herna'ndez, J.G.S., Herna'ndez, S., Antonio, C.G., Ramı'rez, A.B., 2011. Reactive thermally coupled distillation sequences: Pareto front. Ind. Eng. Chem. Res. 50, 926–938. https://doi.org/10.1021/ie101290t.

Grand View Research. Ethyl Levulinate Market Worth $11.8 Million by 2022, March 2016. http://www.grandviewresearch.com/press-release/global-ethyl-levulinate-market (Accessed 13.09.2017).

Harvianto, G.R., Ahmad, F., Lee, M., 2017a. A thermally coupled reactive distillation and pervaporation hybrid process for n-butyl acetate production with enhanced energy efficiency. Chem. Eng. Res. Des. 124, 98–113. https://doi.org/10.1016/j.cherd.2017.05.007.

Harvianto, G.R., Ahmad, F., Lee, M., 2017b. A hybrid reactive distillation process with high selectivity pervaporation for butyl acetate production via transesterification. J. Mem. Sci. 543, 49–57. https://doi.org/10.1016/j.memsci.2017.08.041.

Huber, G.W., Iborra, S., Corma, A., 2006. Synthesis of transportation fuels from biomass: chemistry, catalysts, and engineering. Chem. Rev. 106, 4044–4098. https://doi.org/10.1021/cr068360d.

Joshi, H., Moser, B.R., Toler, J., Smith, W.F., Walker, T., 2011. Ethyl levulinate: a potential bio-based diluent for biodiesel which improves cold flow properties. Biomass Bioenergy 35, 3262–3266. https://doi.org/10.1016/j.biombioe.2011.04.020.

Lee, H.Y., Li, S.Y., Chen, C.L., 2016. Evolutional design and control of the equilibrium-limited ethyl acetate process via reactive distillation-pervaporation hybrid configuration. Ind. Eng. Chem. Res. 55, 8802–8817. https://doi.org/10.1021/acs.iecr.6b01358.

Lin, L.C., 2007. Effects of relative volatility ranking to the design of reactive distillation: excess-reactant design. M.S. Thesis, National Taiwan University, Taipei.

Lipnitzki, F., Field, R.W., Ten, P., 1999. Pervaporation-based hybrid processes: a review of process design, applications and economics. J. Membr. Sci. 153, 183–210. https://doi.org/10.1016/S0376-7388(98)00253-1.

Luyben, W.L., 2009. Control of a column/pervaporation process for separating the ethanol/water azeotrope. Ind. Eng. Chem. Res. 48, 3484–3495. https://doi.org/10.1021/ie801428s.

Nagai, K., 2010. Fundamentals and perspectives for pervaporation. In: Drioli, E., Giorno, L. (Eds.), Comprehensive Membrane Science and Engineering. Elsevier, Oxford, pp. 243–271.

Naidu, Y., Malik, R.K., 2011. A generalized methodology for optimal configurations of hybrid distillation-pervaporation processes. Chem. Eng. Res. Des. 89, 1348–1361. https://doi.org/10.1016/j.cherd.2011.02.025.

Nandiwale, K.Y., Sonar, S.K., Niphadkar, P.S., Joshi, P.N., Deshpande, S.S., Patil, V.S., Bokade, V.V., 2013. Catalytic upgrading of renewable levulinic acid to ethyl levulinate biodiesel using dodecatungstophosphoric acid supported on desilicated H-ZSM-5 as catalyst. Appl. Catal. A Gen. 460, 90–98. https://doi.org/10.1016/j.apcata.2013.04.024.

Novita, F.J., Lee, H.Y., Lee, M., 2015. Self-heat recuperative dividing wall column for enhancing the energy efficiency of the reactive distillation process in the formic acid production process. Chem. Eng. Process.: Process Intensification 97, 144–152. https://doi.org/10.1016/j.cep.2015.09.007.

Novita, F.J., Lee, H.Y., Lee, M., 2017. Energy efficient design of ethyl levulinate reactive distillation process via thermally coupled with external heat-integrated arrangement. Ind. Eng. Chem. Res. 56 (24), 7037–7048. https://doi.org/10.1021/acs.iecr.7b00667.

Oliveira, T.A., Cocchini, U., Scarpello, J.T., Livingston, A.G., 2001. Pervaporation mass transfer with liquid flow in the transition regime. J. Membr. Sci. 183, 119–133. https://doi.org/10.1016/S0376-7388(00)00576-7.

Resk, A.J., Peereboom, L., Kolah, A.K., Miller, D.J., Lira, C.T., 2014. Phase equilibria in systems with levulinic acid and ethyl levulinate. J. Chem. Eng. Data 59 (4), 1062–1068. https://doi.org/10.1021/je400814n.

Sander, U., Soukup, P., 1988. Design and operation of a pervaporation plant for ethanol dehydration. J. Membr. Sci. 36, 463–475. https://doi.org/10.1016/0376-7388(88)80036-X.

Santoso, A., 2010. Design and control of hybrid distillation-membrane systems for separating azeotropic mixtures. M.S. Thesis, National Taiwan University, Taiwan.

Singh, A., Rangaiah, G.P., 2017. Review of technological advances in bioethanol recovery and dehydration. Ind. Eng. Chem. Res. 56, 5147–5163. https://doi.org/10.1021/acs.iecr.7b00273.

Szitkai, Z., Lelkes, Z., Rev, E., Fonyo, Z., 2002. Optimization of hybrid ethanol dehydration systems. Chem. Eng. Process.: Process Intensification 41, 631–646. https://doi.org/10.1016/S0255-2701(01)00192-1.

Tang, Y.R., Chen, Y.W., Huang, H.P., Yu, C.C., Hung, S.B., Lee, M.J., 2005. Design of reactive distillations for acetic acid esterification. AIChE J. 51, 1683–1699. https://doi.org/10.1002/aic.10519.

Taylor, R., Krishna, R., 2000. Modelling reactive distillation. Chem. Eng. Sci. 55, 5183–5229. https://doi.org/10.1016/S0009-2509(00)00120-2.

Triantafyllou, C., Smith, R., 1992. The design and operation of fully thermally coupled distillation columns. Trans. Inst. Chem. Eng. 70A, 118.

Tsai, C.Y., 2014. Kinetic behavior study on the synthesis of ethyl levulinate over heterogeneous catalyst. M.S. Thesis, NTUST, Taiwan.

Tsuchiya, Y., Sumi, K., 1969. Thermal decomposition products of poly (vinyl alcohol). J. Polym. Sci. A-1 Polym. Chem. 7 (11), 3151–3158. https://doi.org/10.1002/pol.1969.150071111.

Tung, S.T., Yu, C.C., 2007. Effects of relative volatility ranking to the design of reactive distillation. Aiche J. 53 (5), 1278–1297. https://doi.org/10.1002/aic.11168.

Turton, R., Bailie, R.C., Whiting, W.B., Shaeiwitz, J.A., 2009. Analysis, Synthesis, and Design of Chemical Processes. Prentice Hall.

Unlu, D., Hilmioglu, N.D., 2016. Synthesis of ethyl levulinate as a fuel bioadditive by a novel catalytically active pervaporation membrane. Energy Fuel 30, 2997–3003. doi: 0.1021/acs.energyfuels.5b02911.

Verhoef, A., Degreve, J., Huybrechs, B., Veen, H.V., Pex, P., Bruggen, B.V.D., 2008. Simulation of a hybrid pervaporation-distillation process. Comput. Chem. Eng. 32, 1135–1146. https://doi.org/10.1016/j.compchemeng.2007.04.014.

Wang, S.J., Lee, H.Y., Ho, J.H., Yu, C.C., Huang, H.P., Lee, M.J., 2010. Plantwide design of ideal reactive distillation processes with thermal coupling. Ind. Eng. Chem. Res. 49, 3262–3274. https://doi.org/10.1016/j.compchemeng.2007.04.01410.1021/ie900786u.

Woods, D.R., 1983. Cost Estimation for the Process Industries. McMaster University, Hamilton, Ontario, Canada.